Electronic Supplementary Material (ESI) for Nanoscale.

SUPPLEMENT INFORMATION

For

Phase stability of the monolayer $Si_{1-x}Ge_x$ with Dirac cone

Xiaoyang Ma[1], Tong Yang[1], Dechun Li[2], Yuan Ping Feng[1,3,*]

[1]Department of Physics, National University of Singapore, 2 Science Drive 3, Singapore 117551

[2]School of Information Science and Engineering, Shandong University, 72 Binhai Road, Qingdao 266237, China

[3]Centre for Advanced 2D Materials, National University of Singapore, 6 Science Drive 2, Singapore 117546

*phyfyp@nus.edu.sg

1. Structures of silicene and germanene

Cluster expansion (CE) simulation and first-principles design of monolayer $Si_{1-x}Ge_x$ are carried out using silicene and germanene as the parent structure. Figure S1 shows the top-, side-views of their atomic structures.

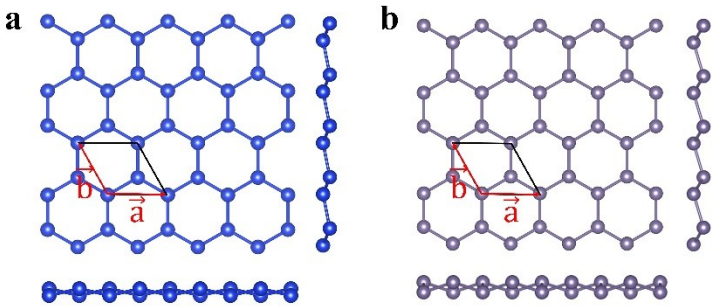

Figure S1: Top-view and side-views of **a** silicene and **b** germanene, respectively. The *x*-axis and the *y*-axis are chosen along the zigzag and armchair direction, respectively. The solid rhombus indicates the unit cell.

2. Effective cluster interactions as a function of the cluster diameter

The ECIs are typically truncated within a cut-off diameter, as their magnitudes tend to diminish with increasing cluster size (the number of lattice points) and range (the distance between the lattice points).

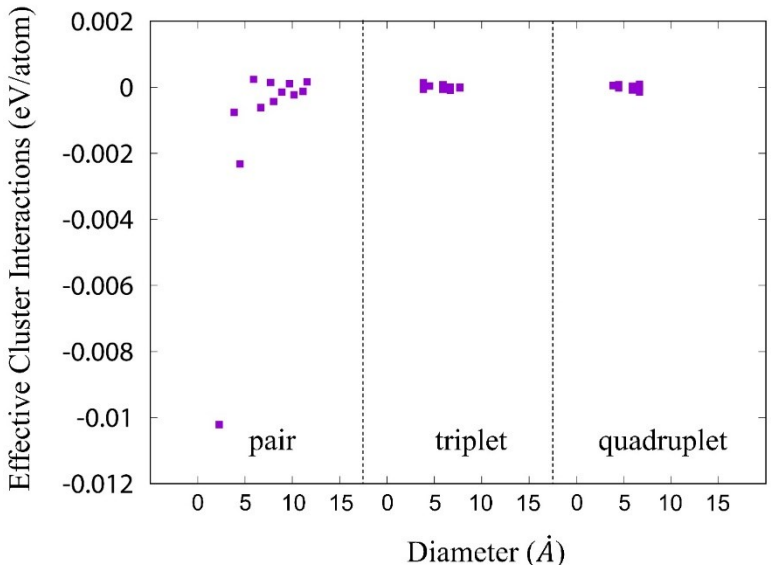

Figure S2: Plot of the effective cluster interactions (ECIs) constructed from the cluster expansion method for $Si_{1-x}Ge_x$ alloy as a function of the cluster diameter. Each point represents a symmetry-unique n-body cluster. The "pair" in the x-axis is nearest-neighbor cluster pair distance for 2-body clusters, "triplet" is nearest-neighbor cluster pair distance for 3-body clusters while "quadruplet" is nearest-neighbor cluster pair distance for 4-body clusters.

3. Quasi-random structures of monolayer $Si_{1-x}Ge_x$ with hexagonal lattice

The random solid solutions with the compositions $x = 0.25, 0.5,$ and 0.75 modeled within 32-atom supercells by using the SQS method. Since the supercell lattice is unrestricted, various lattice can be constructed. Here, we show quasi-random structures with hexagonal lattice that is different from the orthorhombic lattice in main text (Figure 3).

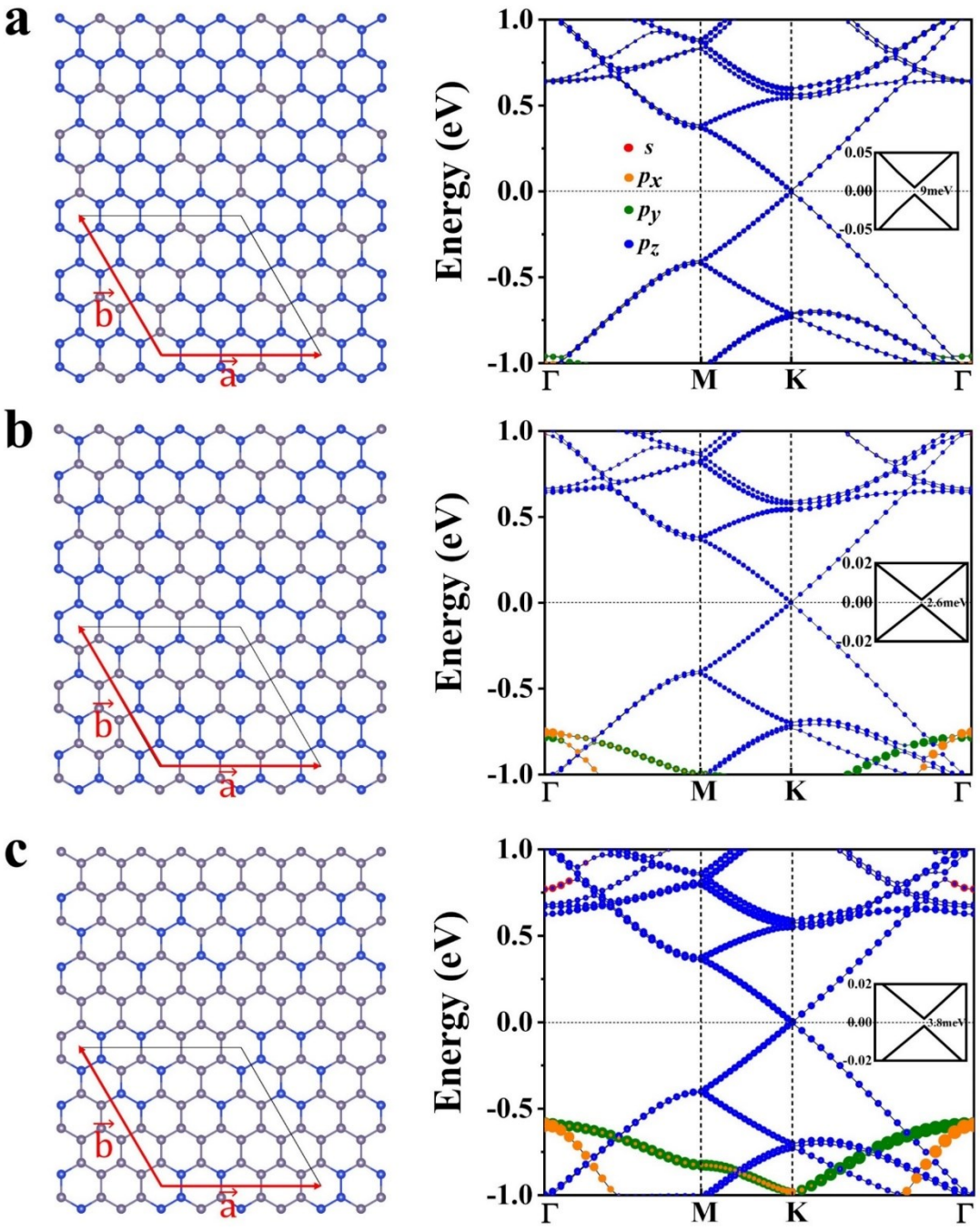

Figure S3: Schematics of the $Si_{1-x}Ge_x$ quasi-random structures and calculated electronic band structure for various compositions, **a** $x = 0.25$, **b** $x = 0.5$ and **c** $x = 0.75$. The blue and grey spheres correspond to Si and Ge respectively. The solid rhombus indicates the unit cell. In band structures, the red, orange, green and blue bubbles represent s, p_x, p_y and p_z orbitals, respectively.

4. Structural data of monolayer $Si_{1-x}Ge_x$ in figure 3.

The lattice constants, bond lengths, and averaged buckling height of silicene, germanene, and monolayer $Si_{1-x}Ge_x$ in figure 3, respectively, are listed in Table S1. The buckling height of silicene is 0.44Å while that of germanene is 0.67Å, which agrees well with the results reported previously [1]. The average buckling heights Δ_{Si-Ge} surprisingly stay the same (0.585 Å) which equals to the buckling amplitude in siligene [2]. Even though the buckling height Δ_{Ge-Ge} shows a decreasing trend with increasing *x,* in contrast to other parameters, it barely affects the average Δ value due to the insensitivity of the Ge-Ge bond to a relatively small strain [3].

	a (Å)	b (Å)	R_{Si-Si}(Å)	R_{Si-Ge}(Å)	R_{Ge-Ge}(Å)	Δ_{Si-Si}(Å)	Δ_{Si-Ge}(Å)	Δ_{Ge-Ge}(Å)	Δ(Å)
Silicene	3.868	3.868	2.277			0.447			0.447
$Si_{0.75}Ge_{0.25}$	7.821	27.065	2.287	2.348	2.409	0.461	0.585	0.702	0.521
$Si_{0.5}Ge_{0.5}$	7.909	27.392	2.294	2.361	2.418	0.479	0.585	0.694	0.586
$Si_{0.25}Ge_{0.75}$	8.005	27.753	2.308	2.366	2.432	0.503	0.585	0.692	0.641
Germanene	4.060	4.060			2.444			0.675	0.675

Table S 1: Structural data of silicene, monolayer $Si_{1-x}Ge_x$ in figure 3, and germanene, including lattice parameter (a and b), bond length (R), and buckling height (Δ), respectively.

5. Mechanical properties of monolayer $Si_{1-x}Ge_x$ with tetragonal lattice

The elastic properties of the SQS generated quasi-random monolayer $Si_{1-x}Ge_x$ in main text are plotted in Figure S4. It is clear the stiffness tensor elements C_{11}, C_{22}, C_{12}, C_{66}, the Young's moduli Y_x and Y_y, the shear modulus S_y decrease monotonically with the Ge content increases.

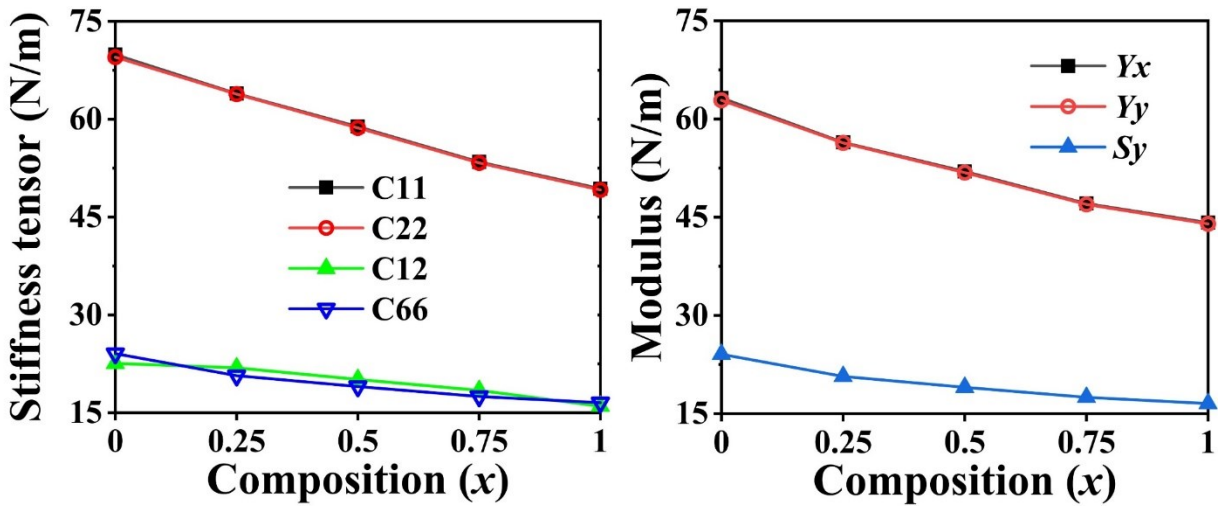

Figure S4: The mechanical properties including stiffness tensor elements $C_{11}, C_{22}, C_{12}, C_{66}$, Young's moduli Y_x and Y_y, and shear modulus S_y of the SQS generated quasi-random monolayer $Si_{1-x}Ge_x$ ($x = 0.25,\ 0.5,$ and 0.75) in main text.

6. Comparison of mechanical properties of $Si_{1-x}Ge_x$ with those of other single atom layers of group 14 elements

The mechanical properties, including the in-plane stiffness C, Young's modulus Y, and Poisson ratios v, obtained in the present work for $Si_{1-x}Ge_x$ are compared those of other single atom layers of group 14 reported in literature, in Table S2. The stable structures are identified as planar (PL) or low-buckled (LB) geometries. It is clear that the in-plane stiffness of planar structures is larger than that of low-buckled structures. Besides, for the buckled structures, the stiffness decreases with increasing buckling height, due to the fact that structures with high buckling height are more susceptible to deformation.

	Geometry	Δ(Å)	$C(N/m)$	$Y(N/m)$	v
Graphene	PL	-	335[4]		0.16[4]
			352[5]	340.8[5]	0.178[5]
			358.1[6]	348[6]	0.169[6]
SiC[4, 7]	PL	-	166[4]	168[7]	0.29[4]
GeC[4]	PL	-	142[4]		0.33[4]
SnC[4]	PL	-	98[4]		0.41[4]
Silicene	LB	0.44[4, 1]	62[4]		0.30[4]
		0.447	68.3[6]	68.1[6]	0.34[6]
			69.90	*63.21*	*0.31*
$Si_{0.75}Ge_{0.25}$	LB	*0.52*	*63.93*	*56.42*	*0.34*
$Si_{0.5}Ge_{0.5}$	LB	*0.586*	*58.88*	*51.99*	*0.34*
GeSi (siligene) [4, 8]	LB	0.55[4]	57[4]		0.32[4]
		0.58[8]	58.64[8]		0.31[8]
$Si_{0.25}Ge_{0.75}$	LB	*0.641*	*53.46*	*46.95*	*0.35*
Germanene	LB	0.64[4, 1]	48[4]		0.33[4]
		0.675	*49.37*	*44.16*	*0.32*
SnSi[4, 8]	LB	0.67[4]	40[4]		0.37[4]
		0.68[8]	41.93[8]		0.35[8]
SnGe[4, 8]	LB	0.73[4]	35[4]		0.38[4]
		0.77[8]	33.26[8]		0.36[8]

Table S2: The mechanical properties including the in-plane stiffness C, Young's modulus Y, and Poisson ratios v for group 14 elemental monolayers and binary compounds. $Si_{0.75}Ge_{0.25}$, $Si_{0.5}Ge_{0.5}$, and $Si_{0.25}Ge_{0.75}$ represent the structures in Figure 3 in the main text. The values in italic are obtained from this work.

7. Monolayer tetragonal SiGe

Use monolayer tetragonal SiGe (t-SiGe) containing pair coupling as an example. Analysis from the tight-binding (TB) model in Ref [9], conduction band (CB) and valence band (VB) of monolayer t-SiGe are mainly constructed by Si-Si antibonding and Ge-Ge bonding states, respectively. To understand the bonding characteristics, the Crystal Orbital Hamilton Populations (COHP) analysis is performed. The negative COHP (-COHP) of the Si-Si and Ge-Ge bond is presented as convention. The positive (negative) value of COHP indicating the

bonding (antibonding) interactions. In Figure S5, it can be seen that VB and CB mainly consist of Ge-Ge bonding states and Si-Si antibonding states, corresponding to the TB picture in Ref [9].

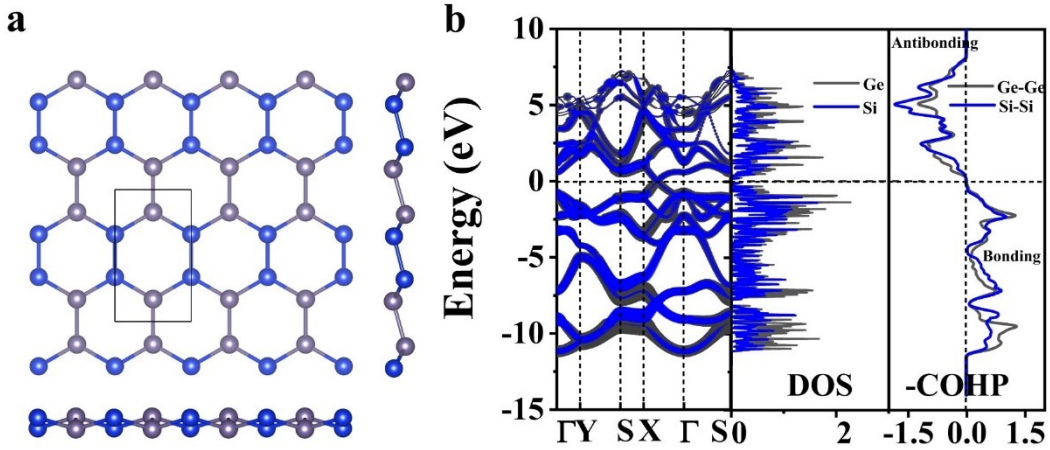

Figure S5: **a** Configuration and **b** calculated electronic properties of monolayer tetragonal SiGe, including band structure with elemental weight (left), projected density of state (middle) and -COHP analysis (right). Grey represents Ge atom and blue represents Si atom.

8. The spin-orbital coupling effect on electronic structure

To investigate the effect of spin-orbit coupling (SOC) on the Dirac cone in $Si_{1-x}Ge_x$, we further calculated the band structures with SOC along X-Γ where Dirac cone appears for SQS-generated $Si_{1-x}Ge_x$ in Figure 3. Figure S6 illustrates the electronic structures with/without SOC. Noticeable SOC induced changes are only found in the valance bands near Γ and around the Dirac point where the degeneracy is lifted and the gap is enlarged. The SOC effect is greater in $Si_{0.25}Ge_{0.75}$ as it increases the bandgap to ~16meV, compared to the small increment of less than 1 meV in $Si_{0.75}Ge_{0.25}$. This can be explained by the greater SOC of germanene (23.9 meV bandgap opening) than silicene (1.55 meV bandgap opening) [10].

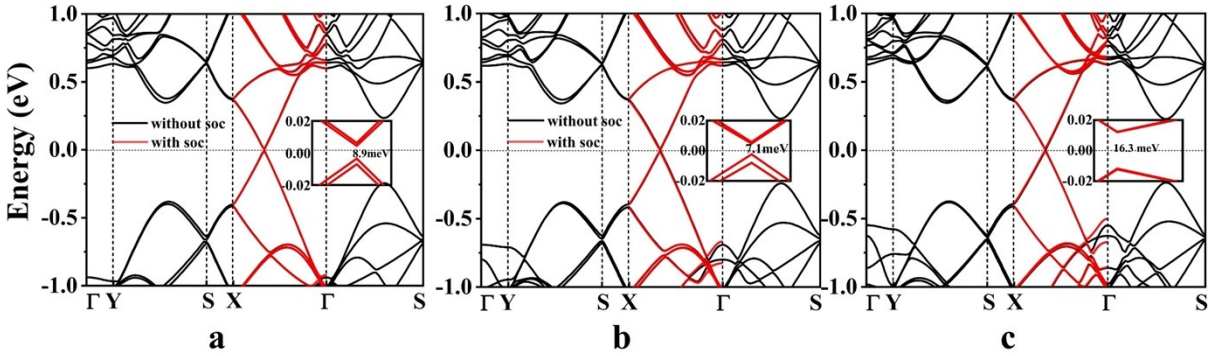

Figure S6: Band structure with (red lines) and without (black lines) SOC of the quasi-random monolayer $Si_{1-x}Ge_x$ alloys at **a** $x = 0.25$, **b** $x = 0.5$ and **c** $x = 0.75$. The inset shows the enlarged band structure near the Dirac point.

References

1. S. Cahangirov, M. Topsakal, E. Aktürk, H. Şahin and S. Ciraci, *Phys. Rev. Lett.*, 2009, **102**, 236804.
2. A. Sannyal, Y. Ahn and J. Jang, *Comput. Mater. Sci.*, 2019, **165**, 121-128.
3. J.-A. Yan, S.-P. Gao, R. Stein and G. Coard, *Phys. Rev. B*, 2015, **91**, 245403.
4. H. Şahin, S. Cahangirov, M. Topsakal, E. Bekaroglu, E. Akturk, R. T. Senger and S. Ciraci, *Phys. Rev. B*, 2009, **80**, 155453.
5. Q. Peng, C. Liang, W. Ji and S. De, *Phys. Chem. Chem. Phys.*, 2013, **15**, 2003-2011.
6. X. Wei, B. Fragneaud, C. A. Marianetti and J. W. Kysar, *Phys. Rev. B*, 2009, **80**, 205407.
7. B. Baumeier, P. Krüger and J. J. P. R. B. Pollmann, 2007, **76**, 085407.
8. J. Shi, Y. Gao, X.-L. Wang and S.-N. Yun, *Chinese Physics Letters*, 2017, **34**, 087701.
9. X. Qin, Y. Liu, X. Li, J. Xu, B. Chi, D. Zhai and X. Zhao, *J. Phys. Chem. Lett.*, 2015, **6**, 1333-1339.
10. C.-C. Liu, W. Feng and Y. Yao, *Phys. Rev. Lett.*, 2011, **107**, 076802.